

RESEARCH PAPER



Phenyl-substituted aminomethylene-bisphosphonates inhibit human P5C reductase and show antiproliferative activity against proline-hyperproducing tumour cells

Giuseppe Forlani^a, Giuseppe Sabbioni^a, Daniele Ragno^b, Davide Petrollino^a and Monica Borgatti^a 

^aDepartment of Life Science and Biotechnology, University of Ferrara, Ferrara, Italy; ^bDepartment of Chemical, Pharmaceutical and Agricultural Sciences, University of Ferrara, Ferrara, Italy

ABSTRACT

In certain cancers, such as breast, prostate and some lung and skin cancers, the gene for the enzyme catalysing the second and last step in proline synthesis, δ^1 -pyrroline-5-carboxylate (P5C) reductase, has been found upregulated. This leads to a higher proline content that exacerbates the effects of the so-called proline-P5C cycle, with tumour cells effectively using this method to increase cell survival. If a method of reducing or inhibiting P5C reductase could be discovered, it would provide new means of treating cancer. To address this point, the effect of some phenyl-substituted derivatives of aminomethylene-bisphosphonic acid, previously found to interfere with the catalytic activity of plant and bacterial P5C reductases, was evaluated *in vitro* on the human isoform 1 (PYCR1), expressed in *E. coli* and affinity purified. The 3,5-dibromophenyl- and 3,5-dichlorophenyl-derivatives showed a remarkable effectiveness, with IC_{50} values lower than 1 μ M and a mechanism of competitive type against both P5C and NADPH. The actual occurrence *in vivo* of enzyme inhibition was assessed on myelogenous erythroleukemic K562 and epithelial breast cancer MDA-MB-231 cell lines, whose growth was progressively impaired by concentrations of the dibromo derivative ranging from 10^{-6} to 10^{-4} M. Interestingly, growth inhibition was not relieved by the exogenous supply of proline, suggesting that the effect relies on the interference with the proline-P5C cycle, and not on proline starvation.

ARTICLE HISTORY

Received 1 February 2021
Revised 9 April 2021
Accepted 15 April 2021

KEYWORDS

Antiproliferative activity;
P5C reductase inhibitors;
proline-P5C cycle; proline-
overproducing tumours

Introduction

Tumour development implies a deep reprogramming of cell metabolism, often inducing some additional or differential metabolic dependencies. These can be exploited for the identification of new therapeutic strategies based on substances able to target specific requirements of malignant cells¹. Among the changes in the metabolic fluxes undergone by tumoral cells to satisfy a larger demand for carbon skeletons, ATP and reducing power, increasing rates of the so-called proline-P5C cycle seem to play a significant role in several cancer types^{2–3}. Although some other mechanisms have been also hypothesised, such as an increase of collagen synthesis and maturation and the acquisition of cancer cell plasticity and heterogeneity⁴, the main contribution of proline metabolism to tumorigenesis seems to rely upon the consequently augmented redox cycling and maintenance of pyridine nucleotides⁵. Proline is synthesised from glutamate or ornithine in short pathways sharing the last step, the NAD(P)H-dependent reduction of the common intermediate δ^1 -pyrroline-5-carboxylic acid (P5C) by P5C reductase (EC 1.5.1.2)⁶. P5C is also formed during the mitochondrial degradation of proline to glutamate, which involves two oxidative steps catalysed in sequence by proline dehydrogenase (ProDH; EC 1.5.5.2)⁷ and P5C dehydrogenase (P5CDH, also known as aldehyde dehydrogenase 4; EC 1.2.1.88)⁸. The former is believed to feed electrons directly to the respiratory ubiquinone pool,⁹ whereas the

latter uses NAD^+ as the electron acceptor¹⁰. The occurrence of a shortcut in which the P5C released by ProDH is not further oxidised by P5CDH, but is reduced back to proline by P5C reductase, has been early hypothesised¹¹. Such apparently futile proline-P5C cycle (Figure 1) may provide the cell with a mechanism for transferring reducing equivalents from the cytosol to the mitochondrion^{11–12}, and to fuel the respiratory chain¹³. Moreover, ProDH activity may alternatively lead to ROS production¹⁴, which can trigger in turn the apoptotic mechanism¹⁵, or increased ATP synthesis for protective autophagy¹⁶. Although in plants the occurrence of the proline-P5C cycle is still a matter of debate due to the physical separation of P5C reductase and ProDH¹⁷, its role in human cell is now well established¹⁸. Consistently, high levels of expression of both ProDH and P5C reductase have been reported in a series of cases in which cell metabolism needs to be enhanced, for instance during nutrient stress¹⁹ or metastasis formation²⁰.

Being highly expressed in several cancer types and possibly linked to tumour cell survival^{2–4,21–23}, the activity of P5C reductase represents a potential target for the development of new therapeutic approaches²⁴. In fact, recent studies on breast²⁵ and prostate²⁶ cancer cell lines demonstrated that P5C reductase knockout was effective in inducing a reduction in tumour size *in vivo* and an increase in cell cycle arrest and apoptosis *in vitro*, respectively. These results would open interesting perspectives through gene

CONTACT Giuseppe Forlani  flg@unife.it  Department of Life Science and Biotechnology, University of Ferrara, Via L. Borsari 46, I-44121 Ferrara (FE), Italy

 Supplemental data for this article can be accessed [here](#).

© 2021 The Author(s). Published by Informa UK Limited, trading as Taylor & Francis Group.

This is an Open Access article distributed under the terms of the Creative Commons Attribution License (<http://creativecommons.org/licenses/by/4.0/>), which permits unrestricted use, distribution, and reproduction in any medium, provided the original work is properly cited.

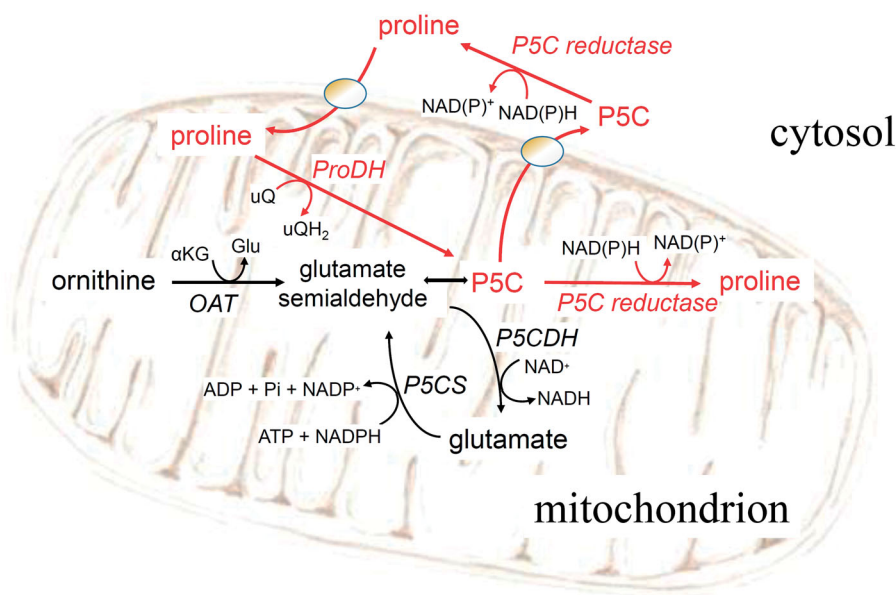


Figure 1. The proline-P5C cycle. Abbreviations that are not listed in the text: OAT: ornithine- δ -aminotransferase; α KG: α -ketoglutarate; Glu: glutamate; P5CS: P5C synthetase; uQ: oxidised ubiquinone; uQH₂: reduced ubiquinone.

therapy, when approved. In the meantime, an amenable approach would be represented by the identification of specific and effective inhibitors of P5C reductase, to be used as antiproliferative agents. A previous screening of a commercially available library of pharmaceutically active compounds pointed out pargylin as a fragment-like hit, with a modest IC₅₀ of 200 μ M, but an encouraging ligand efficiency. The analysis of a number of analogues allowed identifying 4-bromopargyline as the most effective inhibitor, showing an IC₅₀ value of 9 μ M. However, the treatment of cancer cells with the compound resulted in mild effects, with 30–40% reduction of breast cancer cell proliferation at 10 μ M, and an unclear dose-activity relationship on intracellular free proline at higher levels²⁷.

Inhibitors of P5C reductase have been previously exploited as potential herbicides. A preliminary screening *in vitro* pointed out the ability of some aminomethylene bisphosphonic acids to interfere with the activity of the plant enzyme in the micromolar to millimolar range²⁸. Synthesis and analysis of several active derivatives allowed defining the steric and electronic requirements for maintenance or enhancement of the inhibitory properties²⁹, and identifying 3,5-dibromophenyl-aminomethylene bisphosphonic acid as the most effective analogue³⁰. The ability of the latter to inhibit plant growth, and cause the accumulation of P5C levels in treated seedlings, proved that the inhibition of P5C reductase takes place *in vivo*³¹. Moreover, the same compounds were found even more active *in vitro* against P5C reductase of the human pathogen *Streptococcus pyogenes*, although concentrations 2 orders of magnitude higher than IC₅₀ were required to inhibit bacterial growth³². Based on this rationale, we investigated the effectiveness of aminomethylene-bisphosphonic acids in inhibiting human P5C reductase and reducing proliferation of some selected tumour cells lines.

Methods

Substrates, reagents and inhibitors

Unless specified otherwise, all compounds were purchased from Sigma-Aldrich, and were of analytical grade. Δ^1 -pyrroline-5-carboxylic acid was synthesised by the periodate oxidation of δ -allo-

hydroxylysine (Sigma H0377) and purified by cation-exchange chromatography onto a Dowex AG50W-X4 (200–400 mesh) column, as described³³. DL-P5C solutions in 1 M HCl were stored at 4 °C in the dark, and brought to neutral pH just before the assay using proper aliquots of a 1 M Tris base solution. Pargyline (*N*-methyl-*N*-(2-propynyl)benzylamine hydrochloride) was from Sigma (P8013), whereas 4-bromopargyline²⁷ was a generous gift from prof. Reuven Agami (The Netherlands Cancer Institute, Amsterdam, The Netherlands). Phenyl-substituted aminomethylene-bisphosphonic acids were synthesised as described²⁹. For 3,5-dibromophenylaminomethylene-bisphosphonic acid (Br₂PAMBPA) a slightly different procedure was adopted, as it follows.

Procedure for the synthesis of 3,5-dibromophenylaminomethylene-bisphosphonic acid

3,5-Dibromoaniline (3.01 g, 12.00 mmol), triethyl orthoformate (2.40 mL, 14.40 mmol) and diethyl phosphite (6.18 mL, 48.00 mmol) were vigorously stirred and heated at 120 °C for 16 h. After cooling, volatiles were evaporated under reduced pressure. Trituration of the solid with *n*-hexane followed by filtration furnished the pure ester tetraethyl (3,5-dibromophenylaminomethylene) bisphosphonate (4.38 g, 68% yield) which was further dissolved in concentrated hydrochloric acid (300 mL) and refluxed for 4 h. After this period the reaction mixture was cooled and concentrated under reduced pressure affording a solid which was washed with small amounts of cold distilled water and dried under vacuum to obtain the pure bisphosphonic acid Br₂PAMBPA as a whitish solid (3.31 g, 65% overall yield). For NMR analysis ¹H (300 MHz), ¹³C (101 MHz), ³¹P (122 MHz) NMR spectra (Supplementary Figures S1 and S2) were recorded in CDCl₃ or DMSO-*d*₆ solutions at room temperature. The chemical shifts in ¹H and ¹³C NMR spectra were referenced to trimethylsilane (TMS), while in ³¹P NMR were referenced to 85% H₃PO₄ in D₂O. Peak assignments were aided by ¹H-¹H COSY and gradient-HMQC experiments.

Tetraethyl (3,5-Dibromophenylaminomethylene)bisphosphonate: ¹H NMR (300 MHz, CDCl₃) δ = 7.04 (s, 1H, Ar), 6.77 (s, 2H, Ar), 4.35 (bs, 1H, NH), 4.27–4.08 (m, 8H, OCH₂), 4.05 (t, ²J_{H-P} = 22.0 Hz, 1H, CHP₂), 1.32 (t, ¹J_{H-H} = 7.1 Hz, 6H, CH_{3(a)}), 1.28 (t, ¹J_{H-H} = 7.1 Hz,

6H, CH₃(b)); ¹³C NMR (101 MHz, CDCl₃) δ = 148.2 (C, Ar), 124.2 (CH, Ar), 123.4 (2 C, Ar), 115.2 (2 CH, Ar), 63.9 (2 OCH₂(a)), 63.6 (2 OCH₂(b)), 49.9 (t, ¹J_{C-P} = 148.0 Hz, CHP₂), 16.4 (2 CH₃(a)), 16.3 (2 CH₃(b)); ³¹P NMR (122 MHz, CDCl₃) δ = 16.8 (2 P).

3,5-Dibromophenylaminomethylenebisphosphonic acid: ¹H NMR (300 MHz, DMSO-*d*₆) δ = 9.88 (bs, 4H, 4 OH), 6.97 (s, 2H, Ar), 6.81 (s, 1H, Ar), 6.18 (bs, 1H, NH), 3.96 (d, ²J = 22.0 Hz, CHP₂); ¹³C NMR (101 MHz, DMSO-*d*₆) δ = 151.2 (C, Ar), 122.8 (CH, Ar), 120.3 (2 C, Ar), 114.8 (2 CH, Ar), 50.8 (t, ¹J_{C-P} = 140.0 Hz, CHP₂); ³¹P NMR (122 MHz, DMSO-*d*₆) δ = 15.0 (2 P).

Purification of human P5C reductase

The gene coding for P5C reductase 1 (*PYCR1*, gene ID 5831), cloned into the expression vector pET28a⁺³⁴, was kindly provided by prof. Zihao Rao (Tsinghua University, China). For heterologous expression, *E. coli* BL21(DE3) pLysS cells (Invitrogen) were made competent by the calcium chloride method, transformed with the recombinant vector and selected on kanamycin-containing LB plates. About 6 h after inducing gene expression in liquid LB medium at 24 °C by the addition of 1 mM isopropyl-D-thiogalactopyranoside, cells were harvested by centrifugation and stored at -20 °C. Aliquots (about 1 g cell material) were lysed in an ice-cold mortar with 2 g g⁻¹ alumina and resuspended in 20 mL g⁻¹ extraction buffer (50 mM Na phosphate buffer, pH 7.5, containing 200 mM NaCl and 20 mM imidazole). The His-tagged protein was purified from clarified extracts by affinity chromatography onto a His-TrapTM FF column (1 mL, GE Healthcare 17-5319-01). Stepwise elution was achieved by increasing concentrations of imidazole in extraction buffer. Discontinuous SDS-polyacrylamide gel electrophoresis was performed at 8 mA with a 5% stacking and a 12% separating gel, using a Minigel system (BioRad). Samples were mixed with the same volume of 125 mM Tris-HCl buffer (pH 6.8) containing 4% (w/v) SDS, 20% (v/v) glycerol and 10% (v/v) β-mercaptoethanol, and denatured 5 min at 100 °C. Proteins were visualised by soaking gels in Quick Coomassie Stain (CliniSciences) overnight.

P5C reductase assay

Enzyme activity was measured at 30 °C as the P5C-dependent oxidation of NAD(P)H. Assays were performed in 96-microwell plates in a final volume of 0.2 mL. The assay mixture contained 4 mM DL-P5C and 0.5 mM of either NADH or NADPH in 50 mM Tris-HCl buffer, pH 7.5. Parallel blanks were performed in which P5C had been omitted. The decrease of absorbance was measured for 5 min at 0.5-min intervals using a Ledetect plate reader (Labexim, Lengau, Austria) equipped with a LED plugin at 340 nm. Residual NAD(P)H content was estimated on the basis of calibration curves obtained under the same conditions. Activity was calculated by linear regression of data using Prism 6 for Windows, version 6.03 (GraphPad Software, San Diego, CA); one unit of activity was defined as the amount of enzyme that catalyses the P5C-dependent oxidation of 1 nmol NAD(P)H s⁻¹ (nkat). Proteins were measured by the Coomassie Brilliant Blue method³⁵, using bovine serum albumin as the standard. To evaluate substrate affinity, invariable substrates were fixed at the same levels as in the standard assay. For variable substrates, L-P5C ranged from 400 to 2000 μM, while the concentration of NADH and NADPH ranged from 125 to 500 μM. To evaluate the inhibition brought about by pargyline and aminomethylene-bisphosphonates, freshly prepared 10 mM stock solution in water and 100 mM Tris-HCl buffer pH 7.5, respectively, were diluted with water and added to the

reaction mixture before enzyme addition. Parallel control samples were carried out in the absence of any inhibitor. Activity was calculated as described above. Mean activity value in controls was set as 100%, and activity in treated samples was expressed as percent of such value. Percent values were plotted against the logarithm of inhibitor concentration, and data were interpolated using the equation $Y = 100 / (1 + 10^{((\text{Log}[\text{IC}_{50} - X] * \text{HillSlope}))})$. Assays were performed in triplicate (technical replications). Each experiment was repeated at least twice with different enzyme preparations (biological replicates). K_M and V_{max} values, as well as the concentrations causing 50% inhibition (IC_{50}), K_I values and their confidence intervals were estimated by non-linear regression analysis using Prism 6.

Human cell lines and growth conditions

Human myelogenous erythroleukemic K562 cells³⁶ were cultured in a humidified atmosphere of 5% CO₂/air either in complete RPMI 1640 medium (Lonza, Verviers, Belgium) or in a modified medium without L-proline (United States Biological, Massachusetts, USA), both supplemented with 10% foetal bovine serum (FBS; Biowest, Nuaille, France), 100 U mL⁻¹ penicillin and 100 μg mL⁻¹ streptomycin. Human epithelial breast cancer MDA-MB-231 cells³⁷ were cultured under the same conditions in DMEM medium (Lonza, Verviers, Belgium) supplemented with 10% FBS, 100 U mL⁻¹ penicillin, 100 μg mL⁻¹ streptomycin and 2 mM L-glutamine.

Antiproliferative assays

K562 cells in the late exponential phase of growth were seeded in 1 mL medium without FBS in 24-well plates to an initial density of about 20,000 cells mL⁻¹. Treatments with Br₂PAMBPA in the range 1–200 μM were carried out 5 h after seeding. Cell growth was monitored at increasing time after the treatment by determining cell density on 50-μL aliquots with a Z1 Coulter Counter (Coulter Electronics), considering a dimensional range between 8 and 20 μm. MDA-MB-231 cells in the late exponential phase of growth (90% confluence) were washed with sterile PBS, incubated with sterile trypsin-EDTA solution (Sigma-Aldrich, Saint Louis, USA) for 2 min, resuspended in fresh DMEM medium and centrifuged at 1000 g at room temperature for 5 min. Pellets were resuspended in sterile PBS and spun again to remove any residue of trypsin. Cells were finally resuspended in DMEM medium without FBS, and seeded in 24-well plates in a final volume of 1 mL to an initial density of about 20,000 cells mL⁻¹. Treatments with Br₂PAMBPA in the range 1–200 μM were carried out 5 h after seeding, and 2% FBS was added to each well 24 h thereafter. Cell growth was monitored at increasing time after the treatment by destructive harvest. For both cell lines each treatment was carried out at least in triplication, and each experiment was performed at least twice.

Cell viability assay

Cell viability was assessed by the Trypan Blue exclusion test³⁸. Stained cells were counted in a Bürker chamber. Viable and nonviable cells were recorded separately, and the results of three independent counts were pooled. Data were expressed as percent of alive cells.

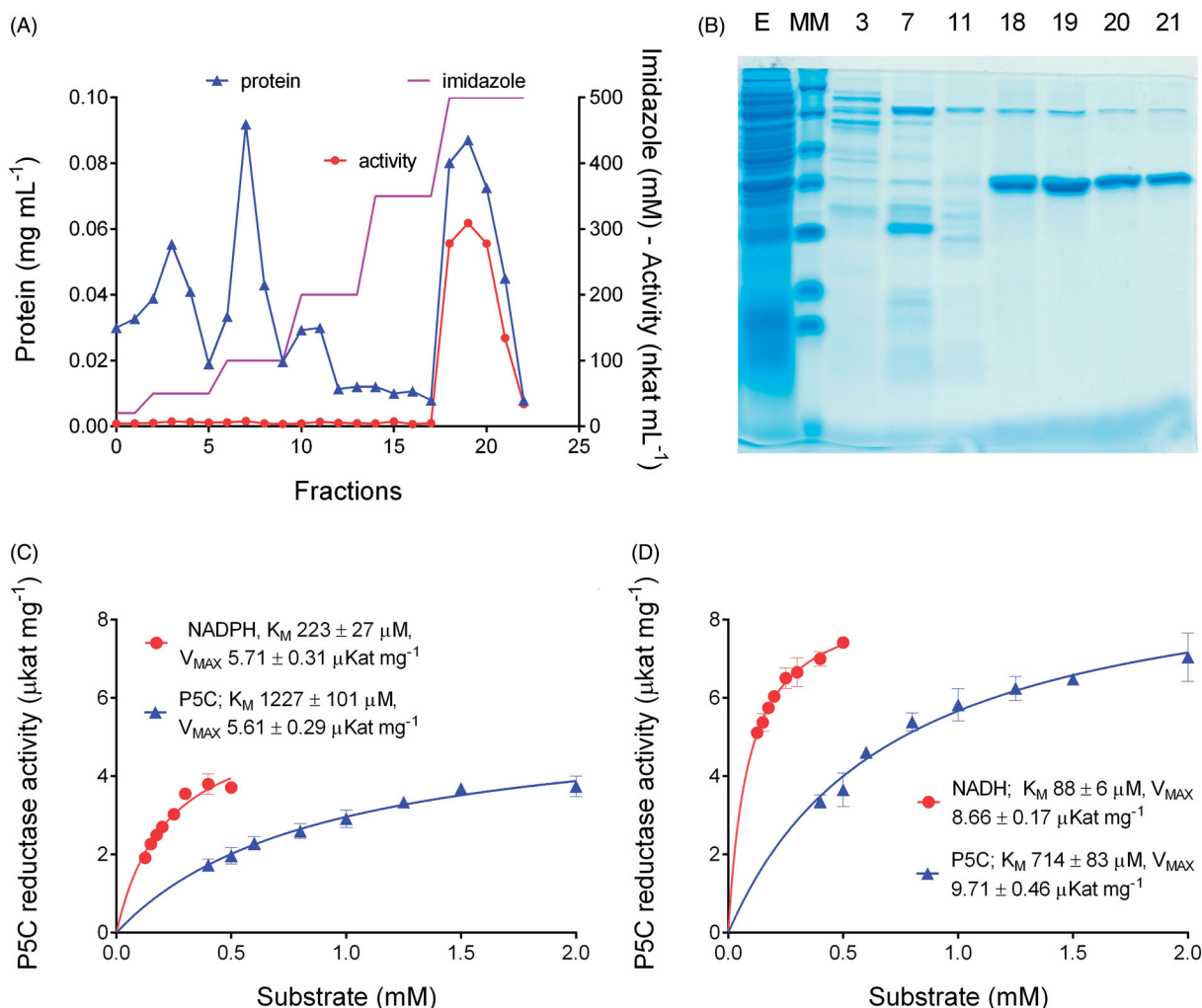


Figure 2. Purification and kinetic characterisation of human P5C reductase. The gene for P5C reductase 1 (*PYCR1*, gene ID 5831) was heterologously expressed in *E. coli*, and the recombinant His-tagged protein was affinity purified by a stepwise gradient of imidazole (panel A). Homogeneity of purified preparations was checked by SDS-PAGE (panel B). Number of lanes in the gel refer to the fractions in panel A; E, crude extract; MM, molecular markers (Fermentas SM0431). Specific activity of the enzyme was measured at varying either substrate, using NADPH (panel C) or NADH (panel D) as the electron donor. Reported data are mean \pm SE over three technical replicates. The whole analysis was repeated with three different enzyme preparations, and similar data were obtained. Both Michaelis-Menten constants and V_{MAX} values pointed at a higher catalytic efficiency with NADH.

Measurement of intracellular free proline and P5C levels

For proline and P5C quantification, treatments were carried out in T-25 flasks containing 10 mL medium. Cells were harvested by centrifugation at 1000 g for 5 min at RT. Each pellet was resuspended in 1.4 mL of sterile PBS and spun again to remove the medium. Washed pellets were transferred on ice, resuspended in a minimal volume of a 3% (w/v) solution of 5-sulfosalicylic acid and subjected to various freeze-thaw cycles to induce rupture of the phospholipid membrane. Cell debris were sedimented by centrifugation at 12,000 g for 5 min at RT, and the supernatants were analysed by the acid ninhydrin method of Williams and Frank, as described³³.

Results

Effect of phenyl-substituted aminomethylenebisphosphonates on the activity of human P5C reductase 1

In order to investigate whether some aminomethylenebisphosphonic acids that had been previously identified as effective inhibitors of plant^{28–31} and bacterial³² P5C reductase have the

potential to inhibit also the human enzyme, P5C reductase-1 was purified through heterologous expression in *Escherichia coli* (Figure 2(A,B)). A stepwise elution protocol with increasing imidazole concentrations allowed resolving the enzyme, with an expected denatured molecular mass of 34.2 kDa, from most contaminating proteins. Only another minor band with a denatured mass of about 70 kDa was evident upon SDS-PAGE analysis, which could be a dimer of P5C reductase itself, as found in other cases^{39–41}. Mean specific activity of the homogeneous enzyme was $2893 \pm 138 \text{ nkat mg}^{-1}$ protein when assayed using NADPH as the electron donor. Activity was not perfectly stable, with a half-life of about 2 weeks at 4 °C (data not shown), yet the amount of protein attainable from a single preparation from 400 mL of induced *E. coli* cells allowed to carry out several thousand assays. A kinetic characterisation of the enzyme was performed to define proper conditions for activity assay (Figure 2(C,D)). Consistently with previous results^{42–44}, data showed a lower K_M and a higher V_{MAX} for NADH. High K_M values for P5C hampered the attainment of completely saturating conditions, especially when NADPH was the co-factor.

Under these optimised experimental conditions, the effect of increasing concentrations of some previously-described inhibitors

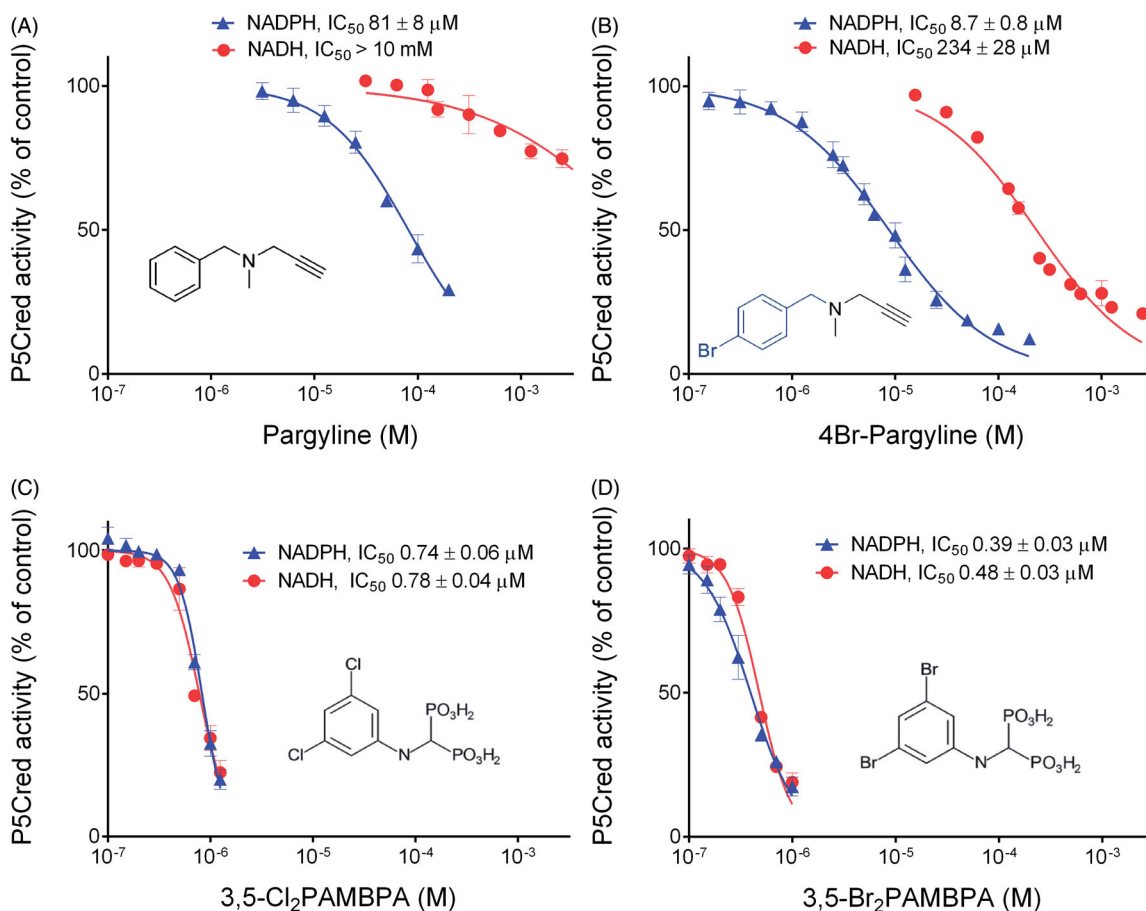


Figure 3. Inhibition of human P5C reductase 1 by pargyline or aminomethylene-bisphosphonates. The purified enzyme was assayed in the presence of increasing concentrations of each compound, as indicated. Parallel controls were carried out in the absence of any inhibitor. Mean activity value in control samples was set as 100%, and activity in treated samples was expressed as percent of such value. Percent values were plotted against the logarithm of inhibitor concentration. Non linear regression of data allowed the calculation of the concentrations causing 50%-inhibition of enzyme activity (IC_{50}). In the case of pargyline (panels A and B), different results were obtained using NADPH or NADH as the electron donor, whereas with aminomethylenebisphosphonic acids (panels C and D) almost overlapping curves were evident. Reported results are mean \pm SE over three technical replicates. The whole experiment was repeated twice with different enzyme preparations, and consistent patterns were obtained.

of human P5C reductase²⁷ was at first assessed. With NADPH as the electron donor, pargyline and 4-bromopargyline confirmed their efficacy (Figure 3(A,B)), with IC_{50} values (81 and 9 μ M, respectively) that were compatible with those (198 and 9 μ M) found hitherto²⁷. A strikingly lower effectiveness was on the contrary evident if NADH was used instead, with IC_{50} values more than one order of magnitude higher (Figure 3(A,B)). When the same experiment was performed with phenyl-substituted aminomethylenebisphosphonates, a remarkably different picture was obtained. Both the 3,5-dichlorophenyl- and the 3,5-dibromophenyl-derivative almost completely suppressed the activity of human P5C reductase at concentrations as low as 1 μ M, and very similar IC_{50} values were found irrespectively of the pyridine dinucleotide used (Figure 3(C,D)). The effect of some other analogues with a different substitution pattern in the phenyl ring³² was also determined. Although several of them were found active in the micromolar range (data not presented), no one showed higher effectiveness than Br₂PAMBPA, which was therefore used for further determinations.

Kinetic analysis of the inhibition brought about by Br₂PAMBPA on human P5C reductase 1

Aminomethylenebisphosphonates had been found to inhibit plant²⁸ and bacterial³² P5C reductases with a mechanism of non

competitive type with respect to NAD(P)H and of uncompetitive type with respect to P5C. To ascertain whether the same holds true for human P5C reductase, a kinetic analysis was performed. Results are summarised in Figure 4. With P5C as the variable substrate, lines converging to the Y-axis in Lineweaver-Burk plots were consistent with an inhibition of competitive type with either NADPH (panel A) or NADH (B) as the electron donor. A similar pattern was obtained at varying NADPH concentration (Figure 4(C)), whereas with NADH results were consistent with a mixed type mechanism of inhibition (Figure 4(D)). A mechanism of competitive type may be an unfavourable feature for an inhibitor, since substrate accumulation *in vivo* might lead to a partial reversal of the inhibitory effect. To take one step further, experiments were therefore carried out to verify whether P5C reductase inhibition by Br₂PAMBPA takes place inside human cells, leading to proline starvation.

Effect of Br₂PAMBPA on the growth of human cancer cell lines

When increasing concentrations of Br₂PAMBPA were added to a modified RPMI medium not containing proline, the growth of human myelogenous leukaemia K562 cells was indeed found to be inhibited in the range from 2 to 200 μ M, with an effect that was proportional to the dose. Inhibition took place 24–36 h following the addition, and 50%-inhibition was achieved at about 20 μ M.

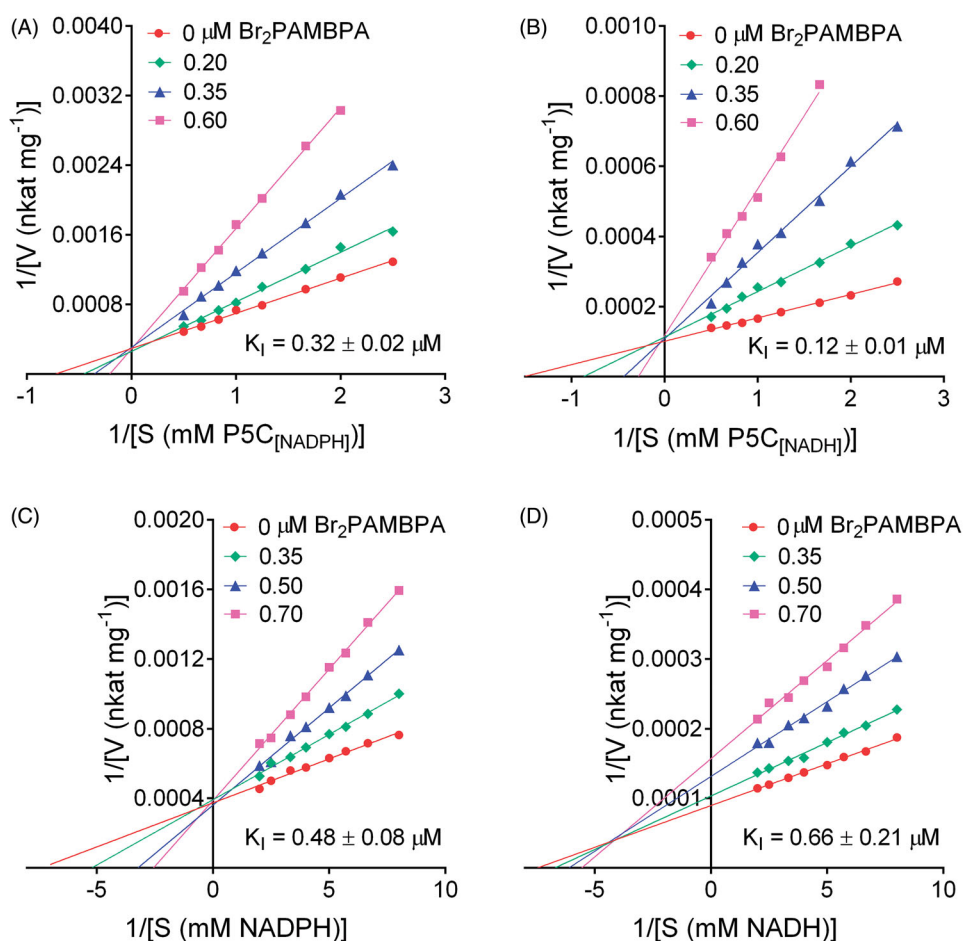


Figure 4. Kinetic analysis of the inhibition of *HsPYCR1* by Br_2PAMBPA . The catalytic rate of the purified enzyme was measured at varying the concentration of a given substrate in the absence or in the presence of increasing levels of the inhibitor. Lines converging to the Y-axis in double reciprocal (Lineweaver-Burk) plots accounted for an inhibition of competitive type against P5C both when using NADPH (panel A) or NADH (panel B) as the electron donor. The same result was evident with respect to NADPH (panel C). On the contrary, with NADH as the variable substrate the pattern was suggestive of an inhibition of mixed-type (panel D). Data are mean over three technical replicates. The whole analysis was repeated three times, and similar patterns were obtained. The reported K_i values are mean \pm SD over replications.

Interestingly, not only the growth rate was slowed down, but treated cells reached a plateau at a lower cell density than untreated controls (Figure 5(A)). Cell viability was significantly reduced at concentrations exceeding $50\ \mu\text{M}$, yet most cells were still alive at doses at which growth had been severely impaired (Figure 5(B)). Remarkably, when the intracellular levels of free proline were quantified, concentrations in treated cultures were not significantly different than in controls (Figure 5(B)), suggesting that the inhibitory effect was not related to proline starvation. Consistently, when the experiment was repeated in unmodified RPMI medium containing $20\ \text{mg L}^{-1}$ ($174\ \mu\text{M}$) Pro, the inhibition was not reversed. On the contrary, a slightly higher effect was evident, with 50% inhibition at about $7\ \mu\text{M}$ (Figure 5(C)), and a more pronounced effect on cell viability (Figure 5(D)). Once again, when free proline content was expressed with respect to viable cells, no reduction was evident up to $50\ \mu\text{M}$, dose at which less than 50% reduction was evident in cells whose proliferation has been almost completely abolished. In all cases, no detectable ($> 1\ \text{nmol [10}^6\ \text{cells]}^{-1}$) levels of P5C were found.

To obtain further evidence, similar experiments were carried out with a breast cancer cell line (MDA-MB-231) in which the inhibition of P5C reductase 1 by small-hairpin RNA had been reported to significantly reduce growth and invasion capabilities⁴⁵. However, in this case cell proliferation strictly required the addition of FBS to DMEM medium, and preliminary experiments

carried out in standard medium showed only mild effects at Br_2PAMBPA concentrations exceeding $50\ \mu\text{M}$ (data not shown). Because such a failure may depend on the interaction between the inhibitor and some FBS components, preventing (or greatly reducing) its uptake by human cells⁴⁶, cell cultures were treated with the bisphosphonate under serum-free conditions, and FBS was added 24 h thereafter. By using this protocol, confirmative results were obtained (Figure 6). Starting from $5\ \mu\text{M}$, both cell growth rate and maximal cell density were progressively reduced, and from $50\ \mu\text{M}$ onward cell proliferation was completely abolished (Figure 6(A)). Almost identical patterns were obtained when the medium was supplemented with $20\ \text{mg L}^{-1}$ Pro, condition under which the growth of untreated controls was slightly speeded up (Figure 6(B)).

Discussion

In human cells, three forms of P5C reductase are present that have specialised roles and different subcellular localizations⁴⁴. The mitochondria-localized PYCR1 is believed to play a main role in the production of proline from glutamate for protein synthesis. PYCR1 has similar K_M s for NADH and NADPH, but a higher reaction rate with NADH, and is competitively inhibited by proline. During recent years, PYCR1 has attracted increasing interest

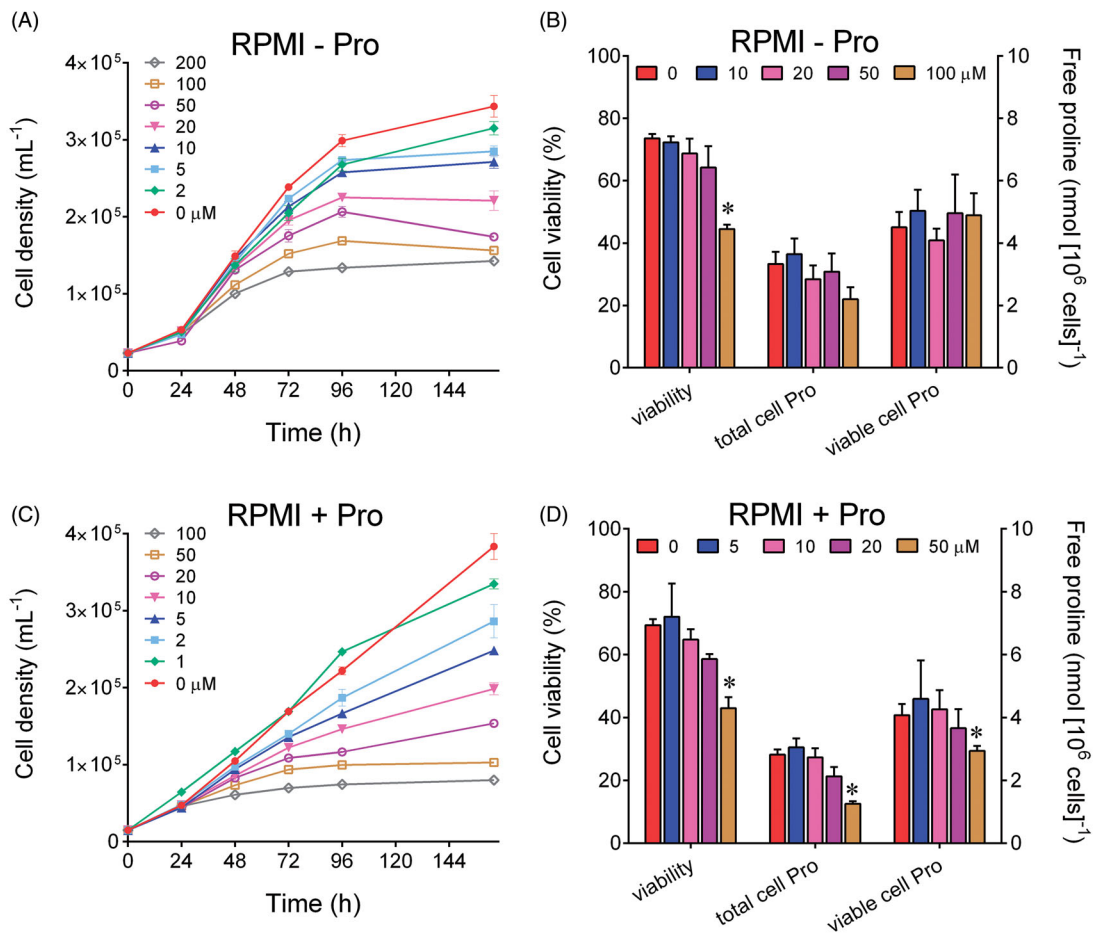


Figure 5. Effect of micromolar levels of Br₂PAMBPA upon the growth of human myelogenous leukaemia K562 cells. The compound was added 5 h after seeding to a modified RPMI medium not containing proline, and the resulting growth was followed until untreated controls reached the early stationary phase (panel A). Cell viability and free proline content were measured by destructive harvest in parallel samples 96 h after the inoculum. Proline concentration was expressed with respect to either total or viable cells (panel B). The same set of determinations was carried out also in unmodified RPMI medium containing 20 mg L⁻¹ Pro (panels C and D). In all cases results are means \pm SD over biological triplicates. Statistical significance of differences between treated and control samples in panels B and D were determined by multiple *t* test using the Holm-Sidak method, with $\alpha = 1.00\%$ (*).

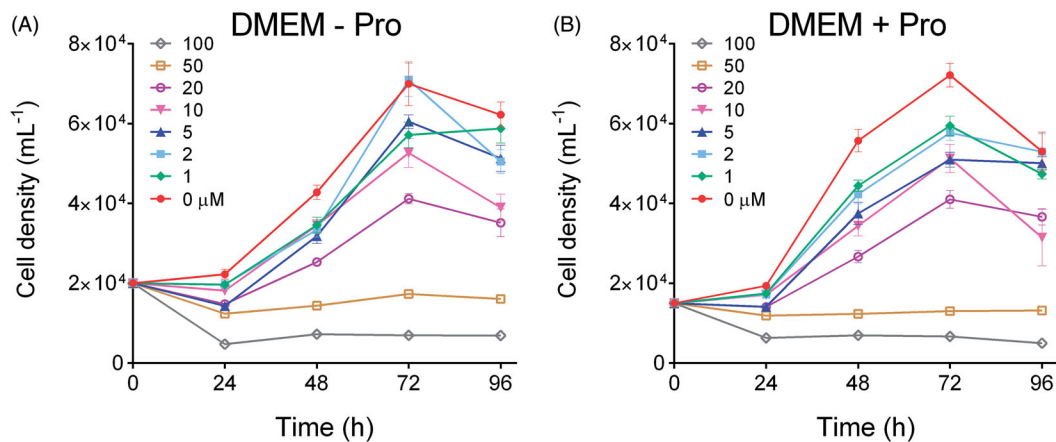


Figure 6. Effect of micromolar levels of Br₂PAMBPA upon the growth of human epithelial breast cancer MDA-MB-231 cells. The compound was added to DMEM medium 5 h after seeding, and 2% FBS was added 24 h thereafter. The resulting growth was followed by destructive harvest until untreated controls reached confluence (panel A). The same experiment was carried out also in DMEM medium supplemented with 20 mg L⁻¹ Pro (panel B). In all cases results are means \pm SE over six biological replicates.

because its upregulation has been found involved in tumour growth and metastatic progression of several types of cancers²⁻⁵. A wide study of mRNA profiles from about two thousand tumours

across 19 different cancer types showed PYCR1 as one of the most consistently overexpressed metabolic genes⁴⁷, and its down-regulation was found to reduce tumour growth and invasion

capabilities, making cancer cells more susceptible to conventional chemotherapeutics⁴⁵. Therefore, P5C reductase represents nowadays an attractive potential target for cancer therapy.

Preliminary results towards the identification of specific inhibitors for human P5C reductase have been recently described, showing 4-bromopargyline as the most effective substance²⁷. However, P5C reductase had been previously exploited as a potential target for herbicides. A long lasting research in our laboratory allowed identifying halogen-substituted derivatives of phenyl-aminomethylene-bisphosphonic acid as potent inhibitors of the plant enzyme^{28–31}. The same compounds were also found to efficiently inhibit the enzyme from a bacterial pathogen³². Their evaluation on human P5C reductase *in vitro*, herein reported, showed an even higher effectiveness, with IC₅₀ values two orders of magnitude lower than those for the plant enzyme, and tenfold lower than that for 4-bromopargyline. Moreover, the same inhibition patterns were found using either NADH or NADPH as the electron donor, whereas in our hands pargyline showed efficacy in the micromolar range only against the NADPH-dependent activity. The higher sensitivity of human P5C reductase corresponded to a different kinetic mechanism. A remarkable difference between the amino acid sequence of the mammal and the plant enzyme does indeed exist, resulting into significant variations in their three-dimensional structure^{6,41} that seem thus to involve the binding site for aminobisphosphonates and influence their interaction. A mechanism of competitive type may represent a drawback, in that substrate accumulation deriving from enzyme inhibition could relieve at least in part the effect of the inhibitors *in vivo*. Confirmative results in a cellular system are thus crucial to support the possibility of using aminomethylene-bisphosphonates to reduce P5C reductase activity inside the cell.

When increasing concentrations of the most active compound were added to the culture medium of two human cancer cell lines, antiproliferative effects were in fact found starting from levels about tenfold higher than IC₅₀ values *in vitro*. This notwithstanding, cell growth was progressively reduced in the range from 2 to 20 μM Br₂PAMBPA, and completely abolished at higher concentrations. Interestingly, even at levels at which proliferation was only slowed down, cell cultures did not attain the same maximal densities than untreated controls, but arrested growth at values that were inversely proportional to the dose. Results obtained with myelogenous leukaemia K562 cells, which grow in suspension to highest densities³⁶, were confirmed with substrate-adhering breast cancer MDA-MB-231 cells that were chosen as a validated system in which PYCR1 is overexpressed and its inhibition causes the reduction of growth and invasion capabilities⁴⁵. In the latter case, the addition of FBS to the medium was found to greatly reduce Br₂PAMBPA effectiveness, most likely as a consequence of inhibitor binding to BSA or other serum components⁴⁶, which may prevent the bisphosphonate from entering the cell. This would represent a serious obstacle for *in vivo* treatments with the compound, yet the problem could be overcome by the adoption of suitable delivery systems⁴⁸.

Interestingly, neither Br₂PAMBPA treatment led to proline starvation, nor the exogenous supply of the amino acid decreased its effectiveness. These results might be consistent with the occurrence of other unrelated target(s) of bisphosphonates in cell metabolism. In fact, the same compounds were found in plants to inhibit also the activity of both cytosolic and plastidial forms of glutamine synthetase, with similar or even higher effectiveness than P5C reductase^{49–50}. However, the possibility that the observed antiproliferative effects may depend on the inhibition of glutamine synthetase is unlikely, since the human enzyme has

been found substantially insensitive to these compounds (IC₅₀ for 3,5-dichlorophenyl-AMPBA of 780 ± 30 μM)⁵¹. Moreover, also phytotoxic effects of these bisphosphonate were found unrelated to proline starvation, which in treated tissues on the contrary accumulated along with the putatively toxic intermediate P5C³¹. Both in control and treated K562 cells P5C was undetectable, and free proline concentration was constant in the range 4–5 nmol (10⁶ cells)⁻¹, levels that were found conserved independently of the presence of exogenous proline in the culture medium, suggesting a strict homeostatic control⁵². Only the treatment with highest Br₂PAMBPA concentrations caused a slight but significant lowering in free proline content. Such results are consistent with those obtained with 4-bromopargyline, whose effect on the intracellular level of proline was not proportional to the dose²⁷.

On the whole, data strongly suggest that the antiproliferative activity of P5C reductase inhibitors is mediated by an interference with the proline-P5C cycle. In this half-biosynthetic, half-catabolic set of reactions, proline is oxidised by ProDH to P5C but the latter, instead of being further oxidised to glutamate in the mitochondrion by P5CDH, is reduced back to proline in the cytosol by P5C reductase (Figure 1). Without resulting in a net change of free proline level, this apparently futile cycle may allow the transfer of reducing equivalents from the cytosol to the mitochondrion, fuelling the respiratory chain^{11–13}. An increased activity of this cycle can improve cancer cell survival, proliferation, and metastasis through a variety of mechanisms ranging from enhanced ATP production, nucleotide synthesis, anaplerosis, and redox homeostasis²⁴. Inhibition of P5C reductase is therefore expected to interfere with all these mechanisms, hampering cell growth even without impacting on proline availability for protein synthesis.

Further information is obviously required to strengthen the possibility of using Br₂PAMBPA or other bisphosphonates for cancer therapy. Next steps will be a deeper insight on the molecular mechanisms fostering cell growth inhibition, the study of the effects against non tumoral cells, and the evaluation of the therapeutic potential in more sophisticated experimental systems. In any case, the availability of specific and effective inhibitors of P5C reductase could help elucidating the functions of the P5C-proline cycle in either physiological or pathological environments. Work is currently in progress with these aims in our laboratory.

Disclosure statement

The authors declare no conflict of interest. The authors alone are responsible for the content and writing of this article.

Funding

This research was supported by grants from the University of Ferrara [FAR 2019].

ORCID

Monica Borgatti  <http://orcid.org/0000-0001-8470-2496>

References

1. Luengo A, Gui DY, Van der Heiden MG. Targeting metabolism for cancer therapy. *Cell Chem Biol* 2017;24:1161–80.

2. Ding Z, Ericksen RE, Escande-Beillard N, et al. Metabolic pathway analyses identify proline biosynthesis pathway as a promoter of liver tumorigenesis. *J Hepatol* 2020;72:725–35.
3. Xiao S, Li S, Yuan Z, Zhou L. Pyrroline-5-carboxylate reductase 1 (PYCR1) upregulation contributes to gastric cancer progression and indicates poor survival outcome. *Ann Transl Med* 2020;8:937.
4. D'Aniello C, Patriarca EJ, Phang JM, Minchiotti G. Proline metabolism in tumor growth and metastatic progression. *Front Oncol* 2020;10:776.
5. Phang JM. Proline metabolism in cell regulation and cancer biology: recent advances and hypotheses. *Antioxid Redox Signal* 2019;30:635–49.
6. Forlani G, Makarova KS, Ruszkowski M, et al. Evolution of plant δ^1 -pyrroline-5-carboxylate reductases from phylogenetic and structural perspectives. *Front Plant Sci* 2015;6:567.
7. Liu W, Phang JM. Proline dehydrogenase (oxidase) in cancer. *Biofactors* 2012;38:398–406.
8. Korasick DA, Končítíková R, Kopečná M, et al. Structural and biochemical characterization of aldehyde dehydrogenase 12, the last enzyme of proline catabolism in plants. *J Mol Biol* 2019;431:576–92.
9. Cabassa-Hourton C, Schertl P, Bordenave-Jacquemin M, et al. Proteomic and functional analysis of proline dehydrogenase 1 link proline catabolism to mitochondrial electron transport in *Arabidopsis thaliana*. *Biochem J* 2016;473:2623–34.
10. Forlani G, Bertazzini M, Zarattini M, Funck D. Functional characterization and expression analysis of rice δ^1 -pyrroline-5-carboxylate dehydrogenase provide new insight into the regulation of proline and arginine catabolism. *Front Plant Sci* 2015;6:591.
11. Hagedorn CH, Phang JM. Transfer of reducing equivalents into mitochondria by the interconversions of proline and δ^1 -pyrroline-5-carboxylate. *Arch Biochem Biophys* 1983;225:95–101.
12. Phang JM. The regulatory functions of proline and pyrroline-5-carboxylic acid. *Curr Top Cell Regul* 1985;25:91–132.
13. Launay A, Cabassa-Hourton C, Eubel H, et al. Proline oxidation fuels mitochondrial respiration during dark-induced leaf senescence in *Arabidopsis thaliana*. *J Exp Bot* 2019;70:6203–14.
14. Hancock CN, Liu W, Alvord WG, Phang JM. Co-regulation of mitochondrial respiration by proline dehydrogenase/oxidase and succinate. *Amino Acids* 2016;48:859–72.
15. Hu CA, Donald SP, Yu J, et al. Overexpression of proline oxidase induces proline-dependent and mitochondria-mediated apoptosis. *Mol Cell Biochem* 2007;295:85–92.
16. Huynh TYL, Zareba I, Baszanowska W, et al. Understanding the role of key amino acids in regulation of proline dehydrogenase/proline oxidase (prodh/pox)-dependent apoptosis/autophagy as an approach to targeted cancer therapy. *Mol Cell Biochem* 2020;466:35–44.
17. Winter G, Todd CD, Trovato M, et al. Physiological implications of arginine metabolism in plants. *Front Plant Sci* 2015;6:534.
18. Liu W, Hancock CN, Fischer JW, et al. Proline biosynthesis augments tumor cell growth and aerobic glycolysis: involvement of pyridine nucleotides. *Sci Rep* 2015;5:17206.
19. Phang JM, Pandhare J, Liu Y. The metabolism of proline as microenvironmental stress substrate. *J Nutr* 2008;138:2008S–15S.
20. Elia I, Broekaert D, Christen S, et al. Proline metabolism supports metastasis formation and could be inhibited to selectively target metastasizing cancer cells. *Nat Commun* 2017;8:15267.
21. Ye Y, Wu Y, Wang J. Pyrroline-5-carboxylate reductase 1 promotes cell proliferation via inhibiting apoptosis in human malignant melanoma. *Cancer Manag Res* 2018;10:6399–407.
22. Cai F, Miao Y, Liu C, et al. Pyrroline-5-carboxylate reductase 1 promotes proliferation and inhibits apoptosis in non-small cell lung cancer. *Oncol Lett* 2018;15:731–40.
23. Wang QL, Liu L. PYCR1 is associated with papillary renal cell carcinoma progression. *Open Med (Wars)* 2019;14:586–92.
24. Tanner JJ, Fendt SM, Becker DF. The proline cycle as a potential cancer therapy target. *Biochemistry* 2018;57:3433–44.
25. Loayza-Puch F, Rooijers K, Buil L, et al. Tumour-specific proline vulnerability uncovered by differential ribosome codon reading. *Nature* 2016;530:490–4.
26. Zeng T, Zhu L, Liao M, et al. Knockdown of PYCR1 inhibits cell proliferation and colony formation via cell cycle arrest and apoptosis in prostate cancer. *Med Oncol* 2017;34:27.
27. Milne K, Sun J, Zaal EA, et al. A fragment-like approach to PYCR1 inhibition. *Bioorg Med Chem Lett* 2019;29:2626–31.
28. Forlani G, Giberti S, Berlicki L, et al. Plant P5C reductase as a new target for aminomethylenebisphosphonates. *J Agric Food Chem* 2007;55:4340–7.
29. Forlani G, Occhipinti A, Berlicki L, et al. Tailoring the structure of aminobisphosphonates to target plant P5C reductase. *J Agric Food Chem* 2008;56:3193–9.
30. Forlani G, Berlicki L, Duò M, et al. Synthesis and evaluation of effective inhibitors of plant δ^1 -pyrroline-5-carboxylate reductase. *J Agric Food Chem* 2013;61:6792–8.
31. Giberti S, Bertazzini M, Liboni M, et al. Phytotoxicity of aminobisphosphonates targeting both δ^1 -pyrroline-5-carboxylate reductase and glutamine synthetase. *Pest Manag Sci* 2017;73:435–43.
32. Forlani G, Petrollino D, Fusetti M, et al. Δ^1 -pyrroline-5-carboxylate reductase as a new target for therapeutics: inhibition of the enzyme from *Streptococcus pyogenes* and effects *in vivo*. *Amino Acids* 2012;42:2283–91.
33. Forlani G, Funck D. A specific and sensitive enzymatic assay for the quantitation of L-proline. *Front Plant Sci* 2020;11:582026.
34. Meng Z, Lou Z, Liu Z, et al. Purification, characterization, and crystallization of human pyrroline-5-carboxylate reductase. *Protein Expr Purif* 2006;49:83–7.
35. Bradford MM. A rapid and sensitive method for the quantitation of microgram quantities of protein utilizing the principle of protein-dye binding. *Anal Biochem* 1976;72:248–54.
36. Klein E, Ben-Bassat H, Neumann H, et al. Properties of the K562 cell line, derived from a patient with chronic myeloid leukemia. *Int J Cancer* 1976;18:421–31.
37. Cailleau R, Olivé M, Cruciger QV. Long-term human breast carcinoma cell lines of metastatic origin: preliminary characterization. *In Vitro* 1978;14:911–5.
38. Crowley LC, Marfell BJ, Christensen ME, Waterhouse NJ. Measuring cell death by trypan blue uptake and light microscopy. *Cold Spring Harb Protoc* 2016;2016. doi: [10.1101/pdb.prot087155](https://doi.org/10.1101/pdb.prot087155)
39. Giberti S, Funck D, Forlani G. Δ^1 -pyrroline-5-carboxylate reductase from *Arabidopsis thaliana*: stimulation or inhibition by chloride ions and feed-back regulation by proline depend on whether NADPH or NADH acts as co-substrate. *New Phytol* 2014;202:911–9.

40. Forlani G, Bertazzini M, Zarattini M, et al. Functional properties and preliminary structural characterization of rice δ^1 -pyrroline-5-carboxylate reductase. *Front Plant Sci* 2015;6:565.
41. Ruskowski MJ, Nocek B, Forlani G, Dauter Z. The structure of *Medicago truncatula* δ^1 -pyrroline-5-carboxylate reductase provides new insights into regulation of proline biosynthesis in plants. *Front Plant Sci* 2015;6:869.
42. Yeh GC, Harris SC, Phang JM. Pyrroline-5-carboxylate reductase in human erythrocytes. *J Clin Invest* 1981;67:1042–6.
43. Lorans G, Phang JM. Proline synthesis and redox regulation: differential functions of pyrroline-5-carboxylate reductase in human lymphoblastoid cell lines. *Biochem Biophys Res Commun* 1981;101:1018–25.
44. Christensen EM, Patel SM, Korasick DA, et al. Resolving the cofactor-binding site in the proline biosynthetic enzyme human pyrroline-5-carboxylate reductase 1. *J Biol Chem* 2017;292:7233–43.
45. Ding J, Kuo M-L, Su L, et al. Human mitochondrial pyrroline-5-carboxylate reductase 1 promotes invasiveness and impacts survival in breast cancers. *Carcinogenesis* 2017;38: 519–31.
46. Zhang Y, Xu YY, Sun WJ, et al. FBS or BSA inhibits EGCG induced cell death through covalent binding and the reduction of intracellular ROS production. *Biomed Res Int* 2016; 2016:5013409.
47. Nilsson R, Jain M, Madhusudhan N, et al. Metabolic enzyme expression highlights a key role for MTHFD2 and the mitochondrial folate pathway in cancer. *Nat Commun* 2014;5: 3128.
48. Das RP, Singh BG, Kunwar A, et al. Tuning the binding, release and cytotoxicity of hydrophobic drug by Bovine Serum Albumin nanoparticles: influence of particle size. *Colloids Surf B Biointer* 2017;158:682–8.
49. Obojska A, Berlicki Ł, Kafarski P, et al. Herbicidal pyridyl derivatives of amino-methylene-bisphosphonic acid inhibit plant glutamine synthetase. *J Agric Food Chem* 2004;52: 3337–44.
50. Occhipinti A, Berlicki Ł, Giberti S, et al. Effectiveness and mode of action of phosphonate inhibitors of plant glutamine synthetase. *Pest Manag Sci* 2010;66:51–8.
51. Kosikowska P, Bochno M, Macegoniuk K, et al. Bisphosphonic acids as effective inhibitors of *Mycobacterium tuberculosis* glutamine synthetase. *J Enz Inh Med Chem* 2016;31:931–8.
52. Hu C-A, Lin WW, Obie C, Valle D. Molecular enzymology of mammalian Δ^1 -pyrroline-5-carboxylate synthase. Alternative splice donor utilization generates isoforms with different sensitivity to ornithine inhibition. *J Biol Chem* 1999;274: 6754–62.